Chemical Science

ROYAL SOCIETY OF CHEMISTRY

EDGE ARTICLE

View Article Online
View Journal | View Issue

Cite this: *Chem. Sci.*, 2022, **13**, 4915

All publication charges for this article have been paid for by the Royal Society of Chemistry

Received 11th February 2022
Accepted 2nd April 2022

DOI: 10.1039/d2sc00876a

rsc.li/chemical-science

Anion-coordination-driven single–double helix switching and chiroptical molecular switching based on oligoureas†

Hongfei Li,‡[a] Lei Kou,‡[a] Lin Liang,[b] Boyang Li,[a] Wei Zhao, *[b] Xiao-Juan Yang[b] and Biao Wu *[ab]

Synthetic foldamers with helical conformation are widely seen, but controllable interconversion amongst different geometries (helical structure and sense) is challenging. Here, a family of oligourea (tetra-, penta-, and hexa-) ligands bearing stereocenters at both ends are designed and shown to switch between single and double helices with concomitant inversion of helical senses upon anion coordination. The tetraurea ligand forms a right-handed single helix upon chloride anion (Cl^-) binding and is converted into a left-handed double helix when phosphate anion (PO_4^{3-}) is coordinated. The helical senses of the single and double helices are opposite, and the conversion is further found to be dependent on the stoichiometry of the ligand and phosphate anion. In contrast, only a single helix is formed for the hexaurea ligand with the phosphate anion. This distinction is attributed to the fact that the characteristic phosphate anion coordination geometry is satisfied by six urea moieties with twelve H-bonds. Our study revealed unusual single–double helix interconversion accompanied by unexpected chiroptical switching of helical senses.

Introduction

Allosteric regulation of DNA helical geometries (helical senses and structures) is tightly associated with gene expression and other cellular processes in biological systems.[1] For example, right-handed B-DNA converts into left-handed Z-DNA during transcription by binding to spermine, spermidine, or metal cations.[2] To mimic these biological processes, considerable advances have been made to regulate single and double helical forms of synthetic foldamers.[3–6] Pioneering work from Lehn and co-workers showed temperature-dependent single–double helix switching based on oligoamides while retaining their left-handed helical sense.[7] Other external stimuli, *e.g.*, solvent,[8–10] light,[11–15] and guest molecules[16–20] have also been shown to regulate single–double helix switching. However, most of these studies have focused on the interconversion between single and double helical forms, and controlling changes in the helical sense along with these processes remains a challenge.

Synthetic foldamers with stimuli-responsive helical sense are promising candidates for chiroptical molecular switches, which are amenable with fabrication of functional materials for data storage.[21–23] As an example, the seminal report on chiroptical molecular switches from Feringa showed the conversion between left- and right-handed configurations of overcrowded chiral alkenes.[24] Triggered by a light source, the chirality of the stereocenter was inversed, thus reversing the helical sense of the pendant foldamers. Besides, anions have also been utilized to regulate helical structures and conformations.[25–30] For example, chiroptical molecular switches based on oligo-indolocarbazole foldamers have been shown to alter their helical senses by anion binding and the solvent effect.[25–27] Very recently, anions were demonstrated to be able to simultaneously regulate single–double helix switching and reversion of helical senses for aryl-triazole based foldamers.[28–30] To the best of our knowledge, this aryl-triazole based foldamer is the only reported example showing the anion-mediated two-in-one switching process involving changes in both the helical structure and helical sense.[12]

In our previous work, we found that *ortho*-phenylene spaced oligoureas display strong coordination affinity toward anions, including chloride and oxoanions.[31–33] Through multiple hydrogen bonds between urea moieties (NH) and anions, the backbones of oligoureas readily wrap around the bound anions in the centers. As the chain length of oligourea increases, single-

[a]*Key Laboratory of Synthetic and Natural Functional Molecule Chemistry of the Ministry of Education, College of Chemistry and Materials Science, Northwest University, Xi'an 710069, China*

[b]*Key Laboratory of Medical Molecule Science and Pharmaceutics Engineering, Ministry of Industry and Information Technology, School of Chemistry and Chemical Engineering, Beijing Institute of Technology, Beijing 102488, China. E-mail: zhaochem@bit.edu.cn; wubiao@bit.edu.cn*

† Electronic supplementary information (ESI) available: Details of syntheses, CD, NMR, mass spectroscopy results and crystal structure. CCDC 2130743–2130746. For ESI and crystallographic data in CIF or other electronic format see https://doi.org/10.1039/d2sc00876a

‡ These authors contributed equally to this work.

strand helical structures are formed by coordinating to two chloride anions.[34] By comparison, oxoanions with higher charges prefer more urea moieties (and therefore hydrogen bonds) in order to stabilize the coordination geometry. For instance, the phosphate anion exhibits a characteristic coordination geometry with six urea moieties through 12 hydrogen bonds, which is easily satisfied in a double helix. Thus, we hypothesize that *ortho*-phenylene spaced oligourea foldamers with a suitable chain length allow for switching of their helical forms by varying the identity of coordinated anions. Yet so far, most of these helical structures are found to be racemic with no preferential helical senses.[35] By introducing a pair of chiral centers, the switching of double-single helical forms and helical senses can be envisioned by coordinating to the phosphate anion.[36–39]

To test this hypothesis, we designed a family of oligourea ligands that incorporate a chiral α-methylbenzyl group at each end to induce single helices with a preferred helical sense.[40–43] It was found that the tetraurea $\mathbf{L^1}$ shows unexpected, different helical structures and helical senses when coordinating to chloride or phosphate anions (Fig. 1). The single-crystal X-ray diffraction and circular dichroism (CD) results unambiguously support a single, right-handed helix (*P*) formed with two chloride anions (LA_2, L: ligand, A: anion) and double, left-handed helices (*MM*) driven by phosphate coordination (L_2A), respectively. In addition, the latter double, left-handed helices can be further switched into a single, right-handed helix (L_1A_1 complex) by interacting with extra phosphate anions.

Results and discussion

Single right-handed helix induced by chloride anion coordination

The details of the syntheses of oligourea ligands $\mathbf{L^1}$, $\mathbf{L^2}$ and $\mathbf{L^3}$ are shown in the ESI.† All the three ligands bear the same α-methylbenzyl chiral group at each end, yet consisting of various numbers of *ortho*-phenylene spaced urea moieties (Fig. 2a). The formation of a folded structure of these ligands upon chloride coordination was first investigated in solution (Fig. 2b). Strong CD signals with a positive Cotton effect were observed for all the three ligands. The structures of the 1 : 2 (ligand to chloride) complexes were confirmed by single-crystal X-ray diffraction

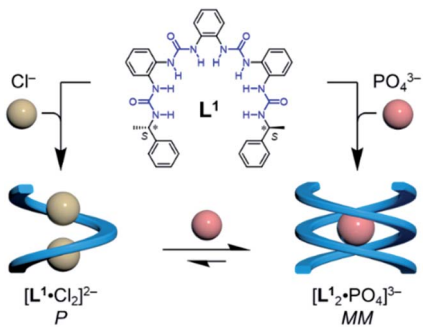

Fig. 1 Formation of single and double helices of the tetraurea ligand $\mathbf{L^1}$ mediated by chloride and phosphate anion binding.

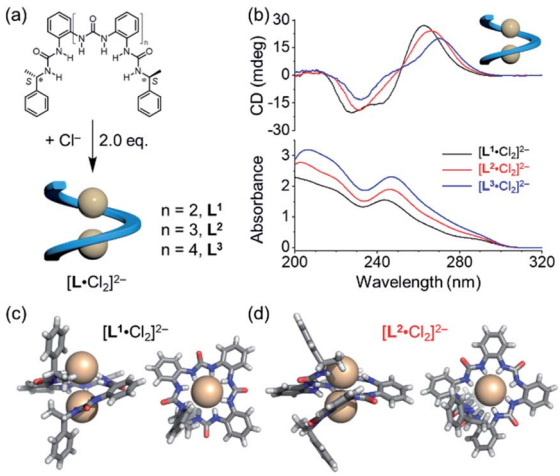

Fig. 2 (a) Structures of ligands $\mathbf{L^1}$–$\mathbf{L^3}$ and their chloride-coordinated single helices $[L{\cdot}Cl_2]^{2-}$. (b) CD and UV-vis spectra of $[L{\cdot}Cl_2]^{2-}$ complexes in acetonitrile ([L] = 30 μM). Crystal structures for the single helices of (c) $[\mathbf{L^1}{\cdot}Cl_2]^{2-}$ and (d) $[\mathbf{L^2}{\cdot}Cl_2]^{2-}$ showing right-handed helical conformation in the solid state (front and top views). Countercations and solvent molecules were omitted for clarity.

(Fig. 2c, d and S2, ESI†), which are consistent with our previous report.[35] As expected, only right-handed conformation was found in the solid state on account of the presence of chiral ending groups. The 1 : 2 complexes were also supported by mass spectrometry analysis (Fig. S19, ESI†).

Consistent with the crystal structures of $[\mathbf{L}{\cdot}Cl_2]^{2-}$ complexes, CD spectra in acetonitrile also support the formation of right-handed helices (Fig. 2b). According to the exciton chirality method,[44–46] the observed pattern of CD signals (positive at long wavelength) is a signature for the formation of right-handed (*P*) helical conformation. This observation suggests that the stereo information of the (*S*) α-methylbenzyl group at both ends is transferred to the folded structures. In addition, the attenuated intensities of CD signals in different oligourea ligands could be attributed to a decrease in the anisotropy factors (*g*-factor) of folded conformations (Fig. S3, ESI†).[47–49] It is worth noting that both CD and UV absorptions are slightly red shifted for $[\mathbf{L^3}{\cdot}Cl_2]^{2-}$ as compared to $[\mathbf{L^1}{\cdot}Cl_2]^{2-}$, which may be attributed to the increased coupling through the oligomer backbone in the longer oligomer.[50]

Double helices induced by phosphate anion coordination and single–double helix switching

Based on the characteristic coordination geometry between *ortho*-phenylene spaced urea moieties and phosphate anions seen in our previous work,[51] we expect to see a different helical structure with phosphate from that with chloride anions. Indeed, instead of forming a single helix as seen with chloride anions, phosphate coordination was found to drive the formation of a double helix with the tetraurea ligand $\mathbf{L^1}$. A similar anion-mediated interconversion of single and double helices has been reported in a previous study of aryl-triazole-based foldamers.[12] In addition to this, we also observed that the helical sense is also inverted from being right-handed for the

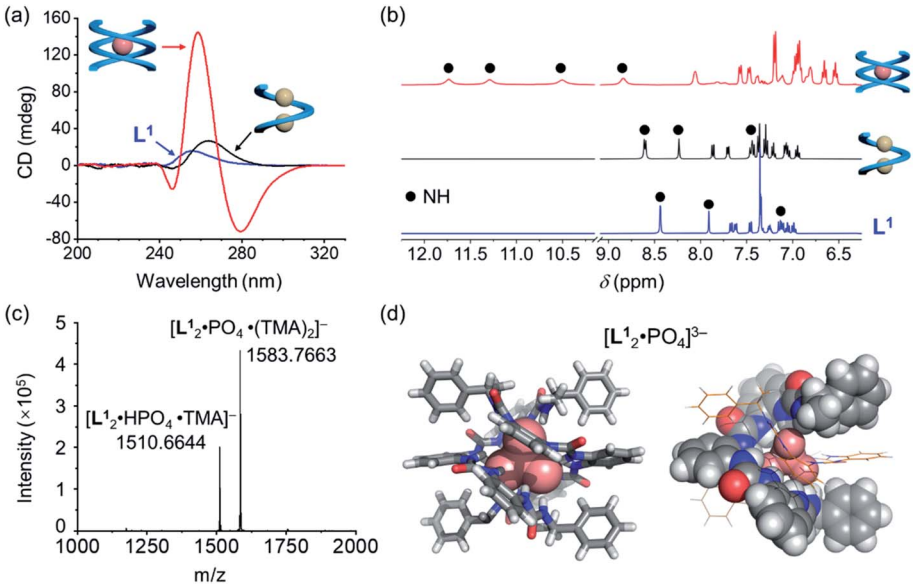

Fig. 3 (a) CD spectra ([L^1] = 30 μM, 5% v/v DMSO/CH_3CN) and (b) stacked partial ^{1}H NMR spectra ([L^1] = 0.6 mM, 400 MHz, DMSO-d_6) of the tetraurea ligand L^1 in its single-helix chloride complex and double-helix phosphate complex. (c) ESI-MS spectrum and (d) crystal structure of the double helical complex $[L^1_2 \cdot PO_4]^{3-}$, tetramethylammonium countercations and solvent molecules were omitted for clarity.

single helix to being left-handed for the double helices, which was usual in previous studies.[52–58]

Inversion of the helical sense from right to left was first shown by CD spectra. We observed a negative Cotton effect in the CD spectrum (negative in a long wavelength region) for the complex of L^1 and phosphate anion (Fig. 3a), indicative of the formation of the left-handed helix as compared to the right-handed helix found with chloride.[59] The CD intensity of the phosphate complex (ΔCD = +145 mdeg at 259 nm) is *ca.* seven times stronger than that of the chloride complex (ΔCD = +22 mdeg at 259 nm), suggesting the formation of a more compact foldamer-anion complex with phosphate than that with the chloride anion.

Considering that the phosphate ion (PO_4^{3-}) with three negative charges is a much stronger hydrogen-bond acceptor than chloride,[60] NMR spectroscopy was used to study these interactions. Larger downfield shifts of N–H (urea) groups were observed compared to the chloride complex (Fig. 3b and S18, ESI†). Specifically, the largest chemical shift change for the N–H peak is about 3.30 ppm (from 8.40 ppm to 11.70 ppm) for the phosphate complex, while only less than 0.33 ppm (7.87 ppm to 8.20 ppm) was seen for the chloride complex (Tables S9 and S10, ESI†). This is consistent with the stronger interactions between the ligand and phosphate than the chloride ion.[61]

To further confirm the stoichiometry of the phosphate complex, we performed mass spectrometry analysis. The major peak in the ESI-MS spectrum is assigned to the L_2A complex, $[L^1_2 \cdot PO_4 \cdot (TMA)_2]^-$ (TMA = tetramethylammonium, Fig. 3c). The single-crystal X-ray diffraction structure confirms the formation of a double, left-handed helix (Fig. 3d and S1, ESI†), in accordance with the strong CD intensities and negative Cotton effect for the tetraurea ligand L^1 with the phosphate anion (Fig. 3a). As shown in the crystal structure, all 16 urea hydrogens (N–H) from the two intertwining ligands form hydrogen bonds with the bound phosphate anion. This coordination number of 16 for phosphate is unusually high in comparison with the typical coordination number of 12 seen in our previous studies.[32]

Addition of 0.5 equivalents of phosphate anions into the solution of $[L^1 \cdot Cl_2]^{2-}$ drives a complete conversion from a single helix to a double helix of $[L^1_2 \cdot PO_4]^{3-}$ (Fig. 4a and S5, ESI†). According to the CD spectra in acetonitrile (Fig. 4b), the positive Cotton effect gradually shifts to the negative pattern by adding phosphate anions. The final CD spectrum is very similar to that by adding 0.5 equivalents of phosphate into the solution of the free tetraurea ligand (Fig. 3a), suggesting the formation of left-handed double helices of the $[L^1_2 \cdot PO_4]^{3-}$ complex. Along

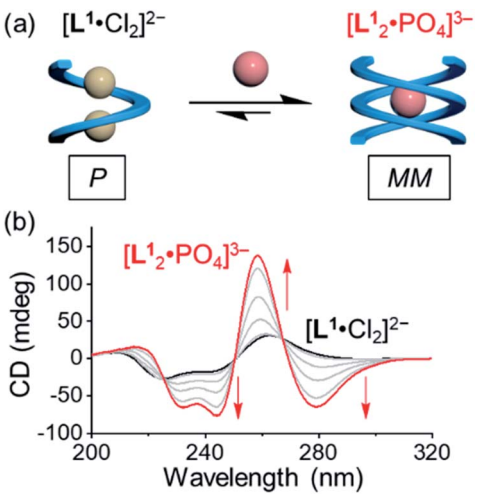

Fig. 4 (a) Schematic representation of the anion-mediated conversion from a single helix to a double helix and (b) the corresponding changes in CD spectra. ([L^1] = 30 μM, CH_3CN).

with change in helical forms, the helical sense is also inverted from being right-handed to being left-handed. This simultaneous dual conversion in both the helical structure and helical sense was rarely seen in previous studies.[62–64] Note that only 0.5 equivalents of phosphate anions are sufficient to fully drive the conversion from the $[\mathbf{L^1}\cdot Cl_2]^{2-}$ complex to $[\mathbf{L^1}_2\cdot PO_4]^{3-}$, inferring once again that the binding affinity of tetraurea ligand $\mathbf{L^1}$ with phosphate is much stronger than that with chloride anions.

Quantitative NMR and UV-vis titration confirms that all oligourea ligands bind to phosphate much strongly than chloride anion (Fig. S6–S17, ESI†). Using ^{1}H NMR titration in DMSO-d_6 (Fig. S12–S14, ESI†), the binding constants of oligoureas $\mathbf{L^1}$, $\mathbf{L^2}$, and $\mathbf{L^3}$ with the chloride ion were determined to be $(2.47 \pm 0.03) \times 10^3$ M^{-1}, $(3.17 \pm 0.06) \times 10^3$ M^{-1}, and $(2.11 \pm 0.04) \times 10^3$ M^{-1}, respectively. In such a polar solvent, 1 : 1 binding mode was applied for chloride coordination. The hexaurea $\mathbf{L^3}$ shows slightly weaker binding affinity compared to the other two ligands, perhaps due to its larger and/or less preorganized cavity for chloride binding. In the case of phosphate, a binding mode of 2 : 1 (L_2A_1) was observed in the titration of oligourea ligands with the phosphate ion (Fig. S15, ESI†). We saw the formation of two distinct complexes (L_2A_1 and L_1A_1), which were supported by the slow exchange between NMR signals during titrations in DMSO-d_6. The binding affinity of phosphate is too high for quantitative determination using NMR measurements. Yet based on changes in the absorbance of UV-vis spectra (Fig. S9–S11, ESI†), we believe that the overall binding affinities of these oligoureas with the phosphate anion are much stronger than those with the chloride anion.

The inversion of the helical sense from a single helix to a double helix is unexpected and unusual. The underlying driving force involved in the transition is not yet clear.[12,26,27,65,66] Flood and co-workers found that the helicity bias between the racemic single helix and chiral double helices for aryl-triazole foldamers is dependent on the anion size.[12] Huc and co-workers found that extra contacts (H-bonds or π–π stacks) among double strands could contribute to the inversion of the helical sense.[66] In our case, based on the crystal structure of $[\mathbf{L^1}\cdot Cl_2]^{2-}$ and $[\mathbf{L^1}_2\cdot PO_4]^{3-}$, we see that the terminal phenyl rings are aligned parallel to the radial direction in the single helix and vertical to the radial direction for the double helix. In the double helix, extra C–H···π contacts (Fig. S1, ESI†) between the terminal phenyl ring and mid-chain phenyl ring are observed, and may help to stabilize the *M*-helicity thus forming left-handed double helices (*MM*). Computational studies (Fig. S23 and S24, ESI†) on the double helix with the opposite right-handed helical sense (*PP*) do not result in similar C–H···π contacts, and so the right-handed structure is suggested to be less stable than the left-handed one. Thus, we postulate that these extra C–H···π contacts in the left-handed double helix are one driving force for the inversion of helicity (Fig. S24, ESI†).

Stoichiometry dependent helix switching induced by phosphate anion coordination

In addition to the anion-mediated interconversion of single and double helices, stoichiometry-controlled helix switching is also observed by further adding phosphate anions (Fig. 5a and S4, ESI†). First, when compared to the mass spectrum of double helices of the phosphate complex, $[\mathbf{L^1}_2\cdot PO_4\cdot(TMA)_2]^-$ (Fig. 3c and S20a, ESI†), the major peaks were assigned to a 1 : 1 complex of $[\mathbf{L^1}\cdot PO_4\cdot(TMA)_2]^-$ when more than one equivalent of phosphate anions were mixed with the tetraurea ligand (Fig. 5b and S20b, ESI†). This is indicative of the conversion from double helices to a single helix. According to the CD signal changes during the titration of double helices with extra phosphate anions in acetonitrile (Fig. 5c and d), we observed consistent shifting of the Cotton effect from being negative to being positive when 0.5 equivalents of phosphate anions were added. The inverted CD signals suggest that the helical sense changed to right-handed. Moreover, the decreased CD intensity also suggests the formation of a less folded structure that is similar to a single helical conformation. The corresponding ^{1}H NMR titration also supports this transformation in solution (Fig. S15, ESI†). When ligand $\mathbf{L^1}$ was mixed with less than 0.5 equivalents of phosphate anions, only one set of peaks were observed, which were assigned to the double helices of the $[\mathbf{L^1}_2\cdot PO_4]^{3-}$ complex. By adding more phosphate anions (up to one equivalent), we observed a decrease in the peaks of the double helix and emergence of a new set of peaks (Fig. S15, ESI†). The ^{1}H NMR spectroscopy results and the CD spectra support stoichiometry-controlled conversion from double helices to a single helix with inversed helical senses.

Given that the phosphate anion typically requires six urea moieties (twelve hydrogen bonds) to satisfy the coordination sphere, we expect to see different helical structures induced by phosphate coordination by increasing the chain length from tetra-urea to penta- and hexa-urea. In particular, the hexaurea ligand $\mathbf{L^3}$ with twelve NH moieties may be able to wrap around one phosphate anion and form a single-strand helix instead of

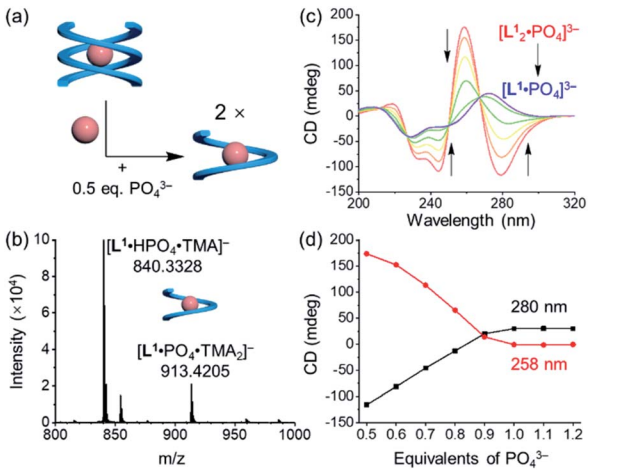

Fig. 5 (a) Schematic representation of the stoichiometry-controlled conversion from double helices to a single helix and conversion of the helical sense from *M* to *P*. (b) ESI-MS spectrum showing the formation of the single helix. (c) CD spectra of $[\mathbf{L^1}_2\cdot PO_4]^{3-}$ by adding 0.5 equivalents of phosphate anions gradually showing conversion in the helical sense. (d) Changes in CD spectra at a wavelength of 258 nm and 280 nm. ($[\mathbf{L^1}] = 30$ μM, CH_3CN).

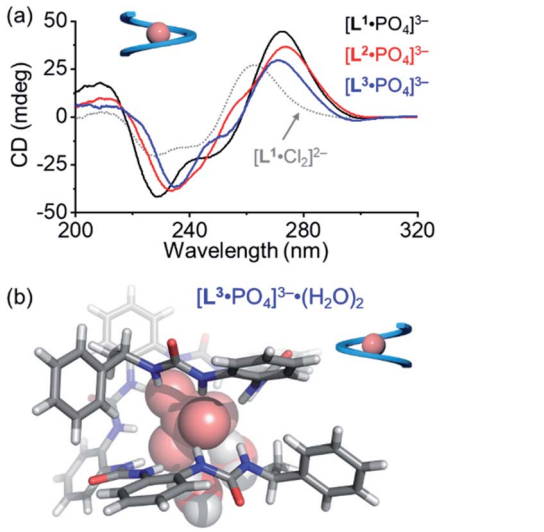

Fig. 6 (a) CD spectra of the single helix of ligands with 1.0 equivalent of phosphate anions. ([L] = 30 μM, CH_3CN) (b) X-ray diffraction crystal structures of the single helix of the $[\mathbf{L^3}\cdot PO_4]^{3-}$ complex. The 1 : 1 complex is shown, and two water molecules are found to interact with the phosphate anion through hydrogen bonding. The tetramethylammonium countercations and solvent molecules were omitted for clarity.

double helices. Indeed, unlike the tetraurea ligand $\mathbf{L^1}$, treating the other two ligands $\mathbf{L^2}$ and $\mathbf{L^3}$ with phosphate anions did not clearly show the transition from a double helix to a single helix (Fig. S16 and S17, ESI†).

For the pentaurea ligand $\mathbf{L^2}$, we observed a set of new peaks when 0.5 equivalents of phosphates were added based on ^{1}H NMR spectra (Fig. S16, ESI†), which is similar to the peaks seen in the case of ligand $\mathbf{L^1}$. However, we did not see a comparable Cotton effect for the double helices (Fig. 3a). Presumably, an intermediate species of an irregular helical structure for the L_2A complex was formed, which readily converted into the single helix $[\mathbf{L^2}\cdot PO_4]^{3-}$ when more phosphate ions were added. The CD spectrum of the $[\mathbf{L^2}\cdot PO_4]^{3-}$ complex in acetonitrile shows a similar Cotton effect to that of the $[\mathbf{L^1}\cdot PO_4]^{3-}$ complex that is assigned to be the right-handed single helix (Fig. 6a).

During the titration of the hexaurea ligand $\mathbf{L^3}$ with the phosphate anion, we only observed the formation of the $[\mathbf{L^3}\cdot PO_4]^{3-}$ complex based on ^{1}H NMR spectra, mass spectrum, and CD spectra (Fig. 6a and S22, ESI†) as a single helix. In addition, the CD signals of the $[\mathbf{L}\cdot PO_4]^{3-}$ complex in acetonitrile also show a similar decreasing tendency to those of the right-handed single helix $[\mathbf{L^1}\cdot Cl_2]^{2-}$, and of the ligands ($\mathbf{L^1}$–$\mathbf{L^3}$) (Fig. 6a). This indicates the formation of the right-handed single helix for all the three $[\mathbf{L}\cdot PO_4]^{3-}$ complexes in solution.

We obtained the crystal structure of the $[\mathbf{L^3}\cdot PO_4]^{3-}$ complex, where to our surprise only a left-handed helix is seen in the solid state (Fig. 6b), which is not consistent with the CD results. This difference could be attributed to specific solvation, and similar solvation-driven inversion of helical senses has been observed before for the oligo-indolocarbazole based foldamers.[26,27,65] In the solid state, two water molecules are seen to interact with the phosphate anion through two hydrogen bonds. This specific solvation affects the orientation of the terminal chiral groups, which is more folded around the phosphate anion than the other oligourea ligands, and thus is more sensitive to what solvates the anions in the solid state. In solution, this coordination geometry with water molecules may not survive, and the right-handed helical conformation is more stabilized just as the other shorter foldamers.

Conclusions

In summary, we report the interconversion of single–double helix structures with simultaneous helical sense switching that is regulated by anion coordination. Based on the characteristic anion coordination ability of *ortho*-phenylene spaced urea moieties, the chloride anion (Cl^-) drives the tetraurea ligand to form a right-handed (*P*) single helix (LA_2 complex) while phosphate (PO_4^{3-}) binding drives the formation of a left-handed (*MM*) double helix (L_2A complex). One equivalent of phosphate anions further converts the double helix into a single helix (LA complex) suggesting stoichiometry dependent single-to-double helix switching. Our study shows a new anion-coordination-mediated approach to the regulation of helical conformations with specific chirality.

Data availability

All experimental and computational data associated with this article are included in the main text and ESI.†

Author contributions

Conceptualization: B. Wu, and H. Li. Data curation: H. Li, B. Li, and L. Kou. Formal analysis: B. Wu, W. Zhao, and H. Li. Investigation: H. Li, L. Kou, and B. Li. Methodology: H. Li, B. Li., and L. Liang. Project administration: H. Li, B. Wu, X.-J. Yang, and W. Zhao. Supervision & funding acquisition: B. Wu, X.-J. Yang, and W. Zhao. Writing (original draft, reviewing & editing): W. Zhao, H. Li, B. Wu, X.-J. Yang, and L. Liang.

Conflicts of interest

The authors declare no competing financial interest.

Acknowledgements

This work was supported by the National Natural Science Foundation of China (91856102, 21772154, 22171023 and 22101024). W. Z. acknowledges the support of the Beijing Institute of Technology Research Fund Program for Young Scholars. We thank the staff of the BL17B beamline at the National Centre for Protein Sciences Shanghai and Shanghai Synchrotron Radiation Facility, Shanghai, People's Republic of China, for assistance during data collection. We also thank Dr Yun Liu and Dr Xiaoyan Zheng for helpful discussions.

Notes and references

1 T. Pawson and P. Nash, *Science*, 2003, **300**, 445–452.
2 A. Rich and S. Zhang, *Nat. Rev. Genet.*, 2003, **4**, 566–572.
3 Y. Ferrand, N. Chandramouli, A. M. Kendhale, C. Aube, B. Kauffmann, A. Grélard, M. Laguerre, D. Dubreuil and I. Huc, *J. Am. Chem. Soc.*, 2012, **134**, 11282–11288.
4 N. Saito, H. Kobayashia and M. Yamaguchi, *Chem. Sci.*, 2016, **7**, 3574–3580.
5 L. R. Holloway, H. H. McGarraugh, M. C. Young, W. Sontising, G. J. O. Beran and R. J. Hooley, *Chem. Sci.*, 2016, **7**, 4423–4427.
6 G. Iadevaia, J. A. Swain, D. Núñez-Villanueva, A. D. Bond and C. A. Hunter, *Chem. Sci.*, 2021, **12**, 10218–10226.
7 V. Berl, I. Huc, R. G. Khoury, M. J. Krische and J.-M. Lehn, *Nature*, 2000, **407**, 720–723.
8 A. Acocella, A. Venturini and F. Zerbetto, *J. Am. Chem. Soc.*, 2004, **126**, 2362–2367.
9 T. Qi, V. Maurizot, H. Noguchi, T. Charoenraks, B. Kauffmann, M. Takafuji, H. Ihara and I. Huc, *Chem. Commun.*, 2012, **48**, 6337–6339.
10 M. Umetani, T. Tanaka and A. Osuka, *Chem. Sci.*, 2018, **9**, 6853–6859.
11 W. Miao, S. Wang and M. Liu, *Adv. Funct. Mater.*, 2017, **27**, 1701368.
12 F. C. Parks, Y. Liu, S. Debnath, S. R. Stutsman, K. Raghavachari and A. H. Flood, *J. Am. Chem. Soc.*, 2018, **140**, 17711–17723.
13 B. Gole, B. Kauffmann, V. Maurizot, I. Huc and Y. Ferrand, *Angew. Chem., Int. Ed.*, 2019, **58**, 8063–8067.
14 S. Pramanik, B. Kauffmann, S. Hecht, Y. Ferrand and I. Huc, *Chem. Commun.*, 2021, **57**, 93–96.
15 N. A. Simeth, S. Kobayashi, P. Kobauri, S. Crespi, W. Szymanski, K. Nakatani, C. Dohno and B. L. Feringa, *Chem. Sci.*, 2021, **12**, 9207–9220.
16 M. Barboiu, G. Vaughan, N. Kyritsakas and J.-M. Lehn, *Chem.–Eur. J.*, 2003, **9**, 763–769.
17 N. Chandramouli, Y. Ferrand, B. Kauffmanncde and I. Huc, *Chem. Commun.*, 2016, **52**, 3939–3942.
18 Q. Gan, X. Wang, B. Kauffmann, F. Rosu, Y. Ferrand and I. Huc, *Nat. Nanotechnol.*, 2017, **12**, 447–452.
19 P. Mateus, N. Chandramouli, C. D. Mackereth, B. Kauffmann, Y. Ferrand and I. Huc, *Angew. Chem., Int. Ed.*, 2020, **59**, 5797–5805.
20 T. Kinoshita, Y. Haketa, H. Maeda and G. Fukuhara, *Chem. Sci.*, 2021, **12**, 6691–6698.
21 B. L. Feringa, R. A. v. Delden, N. Koumura and E. M. Geertsema, *Chem. Rev.*, 2000, **100**, 1789–1816.
22 D. Zhao, T. v. Leeuwen, J. Cheng and B. L. Feringa, *Nat. Chem.*, 2017, **9**, 250–256.
23 N. Ousaka, Y. Takeyama, H. Iida and E. Yashima, *Nat. Chem.*, 2011, **3**, 856–861.
24 B. L. Feringa, N. P. M. Huck and A. M. Schoevaars, *Adv. Mater.*, 1996, **8**, 681–684.
25 J.-m. Suk and K.-S. Jeong, *J. Am. Chem. Soc.*, 2008, **130**, 11868–11869.
26 J.-m. Suk, V. R. Naidu, X. Liu, M. S. Lah and K.-S. Jeong, *J. Am. Chem. Soc.*, 2011, **133**, 13938–13941.
27 D. A. Kim, P. Kang, M.-G. Choi and K.-S. Jeong, *Chem. Commun.*, 2013, **49**, 9743–9745.
28 H. Juwarker, J. M. Lenhardt, D. M. Pham and S. L. Craig, *Angew. Chem., Int. Ed.*, 2008, **47**, 3740–3743.
29 S. Wei, X. Li, Z. Yang, J. Lan, G. Gao, Y. Xue and J. You, *Chem. Sci.*, 2012, **3**, 359–363.
30 Y. Liu, F. C. Parks, W. Zhao and A. H. Flood, *J. Am. Chem. Soc.*, 2018, **140**, 15477–15486.
31 S. Li, M. Wei, X. Huang, X.-J. Yang and B. Wu, *Chem. Commun.*, 2012, **48**, 3097–3099.
32 B. Wu, F. Cui, Y. Lei, S. Li, N. d. S. Amadeu, C. Janiak, Y.-J. Lin, L.-H. Weng, Y.-Y. Wang and X.-J. Yang, *Angew. Chem., Int. Ed.*, 2013, **52**, 5096–5100.
33 X. Zhao, H. Wang, B. Li, W. Zhang, X. Li, W. Zhao, C. Janiak, A. W. Heard, X.-J. Yang and B. Wu, *Angew. Chem., Int. Ed.*, 2022, **61**, e202115042.
34 P. Yang, J. Wang, C. Jia, X.-J. Yang and B. Wu, *Eur. J. Org. Chem.*, 2013, **2013**, 3446–3454.
35 B. Wu, C. Jia, X. Wang, S. Li, X. Huang and X.-J. Yang, *Org. Lett.*, 2012, **14**, 684–687.
36 C. A. Hunter, P. S. Jones, P. M. N. Tigera and S. Tomas, *Chem. Commun.*, 2003, 1642–1643.
37 Y. Wang, J. Xiang and H. Jiang, *Chem.–Eur. J.*, 2011, **17**, 613–619.
38 X. Jin, J. Jiang and M. Liu, *ACS Nano*, 2016, **10**, 11179–11186.
39 W. Zheng, T. Ikai and E. Yashima, *Angew. Chem., Int. Ed.*, 2021, **60**, 11294–11299.
40 E. Yashima, *Nat. Chem.*, 2011, **3**, 12–14.
41 D. Zheng, L. Zheng, C. Yu, Y. Zhan, Y. Wang and H. Jiang, *Org. Lett.*, 2019, **21**, 2555–2559.
42 G. N. Vemuri, R. R. Pandian, B. J. Spinello, E. B. Stopler, Z. J. Kinney and C. S. Hartley, *Chem. Sci.*, 2018, **9**, 8260–8270.
43 C. A. Hunter, A. Spitaleri and S. Tomas, *Chem. Commun.*, 2005, **29**, 3691–3693.
44 D. Gargiulo, N. Ikemoto, J. Odingo, N. Bozhkova, T. Iwashita, N. Berova and K. Nakanishi, *J. Am. Chem. Soc.*, 1994, **116**, 3760–3767.
45 T. Taniguchi and K. Monde, *J. Am. Chem. Soc.*, 2012, **134**, 3695–3698.
46 J. Chen, A. J. Ferreira and C. M. Beaudry, *Angew. Chem., Int. Ed.*, 2014, **53**, 11931–11934.
47 I. Dolamic, S. Knoppe, A. Dass and T. Bürgi, *Nat. Commun.*, 2012, **3**, 798.
48 J. Yao, W. Wu, W. Liang, Y. Feng, D. Zhou, J. J. Chruma, G. Fukuhara, T. Mori, Y. Inoue and C. Yang, *Angew. Chem., Int. Ed.*, 2017, **56**, 6869–6873.
49 J. Hao, H. Lu, L. Mao, X. Chen, M. C. Beard and J. L. Blackburn, *ACS Nano*, 2021, **15**, 7608–7617.
50 B. Li, B. Zheng, W. Zhang, D. Zhang, X.-J. Yang and B. Wu, *Cryst. Growth Des.*, 2019, **19**, 6527–6533.
51 R. Li, Y. Zhao, S. Li, P. Yang, X. Huang, X.-J. Yang and B. Wu, *Inorg. Chem.*, 2013, **52**, 5851–5860.
52 C. Dolain, V. Maurizot and I. Huc, *Angew. Chem., Int. Ed.*, 2003, **42**, 2738–2740.

53 T. Miyagawa, A. Furuko, K. Maeda, H. Katagiri, Y. Furusho and E. Yashima, *J. Am. Chem. Soc.*, 2005, **127**, 5018–5019.
54 K. Okoshi, S.-i. Sakurai, S. Ohsawa, J. Kumaki and E. Yashima, *Angew. Chem., Int. Ed.*, 2006, **45**, 8173–8176.
55 S.-i. Sakurai, K. Okoshi, J. Kumaki and E. Yashima, *J. Am. Chem. Soc.*, 2006, **128**, 5650–5651.
56 D. Pijper and B. L. Feringa, *Angew. Chem., Int. Ed.*, 2007, **46**, 3693–3696.
57 I. Louzao, J. M. Seco, E. Quiñoá and R. Riguera, *Angew. Chem., Int. Ed.*, 2010, **49**, 1430–1433.
58 F. Freire, J. M. Seco, E. Quiñoá and R. Riguera, *Angew. Chem., Int. Ed.*, 2011, **50**, 11692–11696.
59 N. Berova, L. D. Bari and G. Pescitellib, *Chem. Soc. Rev.*, 2007, **36**, 914–931.
60 C. Jia, B. Wu, S. Li, Z. Yang, Q. Zhao, J. Liang, Q.-S. Li and X.-J. Yang, *Chem. Commun.*, 2010, **46**, 5376–5378.
61 J. Zhao, D. Yang, Y. Zhao, X.-J. Yang, Y.-Y. Wang and B. Wu, *Angew. Chem., Int. Ed.*, 2014, **53**, 6632–6636.
62 P. A. Korevaar, S. J. George, A. J. Markvoort, M. M. J. Smulders, P. A. J. Hilbers, A. P. H. J. Schenning, T. F. A. D. Greef and E. W. Meijer, *Nature*, 2012, **481**, 492–496.
63 H. Liang, B. Hua, F. Xu, L.-S. Gan, L. Shao and F. Huang, *J. Am. Chem. Soc.*, 2020, **142**, 19772–19778.
64 J. S. S. K. Formen and C. Wolf, *Angew. Chem., Int. Ed.*, 2021, **60**, 27031–27038.
65 H. J. Lee, H.-G. Jeon and K.-S. Jeong, *Supramol. Chem.*, 2014, **27**, 378–385.
66 Q. Gan, Y. Ferrand, N. Chandramouli, B. Kauffmann, C. Aube, D. Dubreuil and I. Huc, *J. Am. Chem. Soc.*, 2012, **134**, 15656–15659.